Int. J. of Applied Mechanics and Engineering, 2022, vol.27, No.1, pp.91-106
DOI: 10.2478/ijame-2022-0007

DIFFERENCE SCHEME FOR DIFFERENTIAL-DIFFERENCE PROBLEMS WITH SMALL SHIFTS ARISING IN COMPUTATIONAL MODEL OF NEURONAL VARIABILITY

Mamatha KODIPAKA
Department of Mathematics, Vardhaman College of Engineering, Shamshabad, Hyderabad, INDIA

Siva Prasad EMINENI and Phaneendra KOLLOJU*
Department of Mathematics, University College of Science, Osmania University, Hyderabad, INDIA
E-mail: kollojuphaneendra@yahoo.co.in

The solution of differential-difference equations with small shifts having layer behaviour is the subject of this study. A difference scheme is proposed to solve this equation using a non-uniform grid. With the non-uniform grid, finite - difference estimates are derived for the first and second-order derivatives. Using these approximations, the given equation is discretized. The discretized equation is solved using the tridiagonal system algorithm. Convergence of the scheme is examined. Various numerical simulations are presented to demonstrate the validity of the scheme. In contrast to other techniques, maximum errors in the solution are organized to support the method. The layer behaviour in the solutions of the examples is depicted in graphs.

Key words: non-uniform grid, differential-difference equation, boundary layer.

1. Introduction

The analysis of differential-difference equations with small shifts and layer behaviour has progressed rapidly in recent years. Simulation of complicated physical systems requires the use of differential-difference equations. These equations are used in the modelling of a variety of real-world situations, such as population dynamics [1], physiological process reproductions [2], predator-prey models [3] and the production of an action potential in nerve cells by random synaptic inputs in dendrites [4]. The mathematical details of these problems are referred to in [5, 6].

In [4], the author discussed a problem with stochastic effects caused by neuron excitation. The determination by random synaptic inputs into the dendrites of the expected time to generate action potential in nerve cells can be modelled to constitute a first-time problem. In this model, the input distribution is seen as an exponential decay Poisson process. If inputs with the variance parameter σ and drift parameter μ are also available to be modelled as a Wiener process, then the problem can be defined as a linear second order differential-difference equation with the initial membrane potential for expected first-exit time $\theta(s)$, $s \in (s_1, s_2)$ and can be formulated as

$$\frac{\sigma^2}{2}\theta''(s)+(\mu-s)\theta'(s)+\lambda_e\theta(s+a_e)+\lambda_i\theta(s-a_i)-(\lambda_e+\lambda_i)\theta(s)=-1 \tag{1.1}$$

where the values $s = s_1$ and $s = s_2$ correspond to the inhibitory reversal potential and to the threshold value of the membrane potential for action potential generation respectively. Here the term $-s\theta'(s)$ represents the

* To whom correspondence should be addressed

exponential decay between synaptic inputs. The undifferentiated term corresponds to excitatory and inhibitory synaptic inputs, modelled as a Poisson process with rates λ_e and λ_i, respectively, and produce jumps in the membrane potential of amounts a_e and a_i, respectively, which are small quantities and could be dependent on voltage. The boundary condition is $\theta(s)=0,\ s\notin(s_1,\ s_2)$.

The numerical treatment of singularly perturbed differential-difference equations is far from trivial because the solution to these problems varies rapidly in some parts and slowly in some other parts. Also, the layer profile varies according to the values of the delay and advance parameters. Hence, to solve these problems, we required more efficient, simpler computational techniques.

The analysis and numerical methodology of singular perturbation problems (SPPs) are presented in [7, 8, 9, 10, 11]. The authors in [12, 13] used the Taylor approximation to implement a parameter-uniform differential scheme to solve a model based on neural variability. In [14], the authors investigated turning point behaviour in differential-difference equations. Researchers compared layer behaviour for various shift parameter values in [15], focusing on solutions that display layer behaviour at one or both ends of the boundary. The same authors expanded their research in [16], revealing that fast oscillation solutions are more prone to small delays than layer solutions based on the WKB approach.

The authors in [17] proposed a finite difference technique to transform the time fractional stochastic KdV equation into elliptic stochastic differential equations. Then, the resulting elliptic SDEs were solved using a meshless method based on radial basis functions. In [18], the researchers suggested a finite difference scheme and radial basis functions interpolation to convert the solution of time-fractional stochastic advection–diffusion equations to the solution of a linear system of algebraic equations. In [19], a new scheme employing a collocation method in combination with matrices of Fibonacci polynomials is introduced for the solution of singularly perturbed differential-difference equations.

Sirisha *et al.* [20] addressed the mixed shifts problem by decomposing the domain and applying a mixed difference technique. Phaneendra *et. al.* [21] employed numerical integration with interpolation to solve equations containing a layer or oscillatory nature. In [22], researchers proposed a fitted spline approach for solving the delay problem with a layer at one end of the domain. Based on the triangular function theorem, in [23], the authors proposed a set of finite difference methods for convention-diffusion equations, which is subsequently extended to solve two-dimensional problems using the AID methodology.

2. Description of the problem

The differential-difference equation describing layer behaviour is

$$\varepsilon\theta''(s)+p(s)\theta'(s)+q(s)\theta(s-\delta)+r(s)\theta(s)+v(s)\theta(s+\eta)=f(s) \tag{2.1}$$

on $(0,1)$, under the boundary conditions

$$\theta(s)=\varphi(s) \quad \text{on} \quad -\delta\le s\le 0, \quad \theta(s)=\gamma(s) \quad \text{on} \quad 1\le s\le 1+\eta \tag{2.2}$$

where $0<\varepsilon<<1$ is a perturbation parameter $p(s),\ q(s),\ r(s),\ v(s),\ f(s),\ \varphi(s)$ and $\gamma(s)$ are the smooth functions and $0<\delta=o(\varepsilon),\ 0<\eta=o(\varepsilon)$ are the delay and the advance parameter, respectively. The solution of Eq.(2.1) with Eq.(2.2) exposes a layer at the left end of the domain if $p(s)-\delta q(s)+\eta v(s)>0$ and a layer at the right end of the domain if $p(s)-\delta q(s)+\eta v(s)<0$. If $p(s)=0$, then the problem has oscillatory solution or two layers depending upon the cases whether $q(s)+r(s)+v(s)$ is positive or negative.

Since the solution $\theta(s)$ of Eq.(2.1) is suitably differentiable, the terms $\theta(s-\delta)$ and $\theta(s+\eta)$ $\theta(s-\eta)$ can be expanded using the Taylor series, then we have:

$$\theta(s-\delta)\approx\theta(s)-\delta\theta'(s), \qquad \theta(s+\eta)\approx\theta(s)+\eta\theta'(s). \tag{2.3}$$

Using Eq.(2.3) in Eq.(2.1), we get:

$$\varepsilon\theta''(s)+a(s)\theta'(s)+b(s)\theta(s)=f(s). \tag{2.4}$$

Equation (2.4) is a second-order SPP. Here,

$$a(s)=p(s)-\delta q(s)+\eta v(s), b(s)=q(s)+r(s)+v(s).$$

3. Derivation of the scheme

Let the advance parameter be in $[0,1]$. Let $s_0=0,\ s_i=\sum_{k=0}^{i-1}h_k\ (1\le i\le N)$.

$h_k=s_{k+1}-s_k$, $s_N=1$ and $d_i=h_i-h_{i-1}$ be the common grid difference.

Using the Taylor series expansion of θ_{i+1} & θ_{i-1} and ignoring the term of the third and higher order, we get

$$\theta_{i+1}\approx\theta_i+h_i\theta_i'+\frac{h_i^2}{2}\theta_i'', \tag{3.1}$$

$$\theta_{i-1}\approx\theta_i-h_{i-1}\theta_i'+\frac{h_{i-1}^2}{2}\theta_i''. \tag{3.2}$$

Multiplying Eq.(3.2) by $\frac{d_i}{h_{i-1}}$, we get:

$$\frac{d_i}{h_{i-1}}\theta_{i-1}=\frac{d_i}{h_{i-1}}\theta_i-d_i\theta_i'+\frac{d_i h_{i-1}}{2}\theta_i''. \tag{3.3}$$

Summing Eq.(3.1), Eq.(3.2) and Eq.(3.3) gives:

$$\theta_i''=\frac{2}{h_i(h_i+h_{i-1})}\left(1+\frac{d_i}{h_{i-1}}\right)\theta_{i-1}-\left(2+\frac{d_i}{h_{i-1}}\right)\theta_i+\theta_{i+1}. \tag{3.4}$$

Using Eq.(3.1) and Eq.(3.2), we have:

$$\theta_i'=\frac{1}{h_i+h_{i-1}}\left\{(\theta_{i+1}-\theta_{i-1})-\frac{d_i}{h_i}\left[\left(1+\frac{d_i}{h_{i-1}}\right)\theta_{i-1}-\left(2+\frac{d_i}{h_{i-1}}\right)\theta_i+\theta_{i+1}\right]\right\}. \tag{3.5}$$

Using Eq.(3.4) and Eq.(3.5) in Eq.(2.4), we get:

$$\left\{\begin{array}{l}\dfrac{2\varepsilon}{h_i(h_i+h_{i-1})}\left[\left(1+\dfrac{d_i}{h_{i-1}}\right)\theta_{i-1}-\left(2+\dfrac{d_i}{h_{i-1}}\right)\theta_i+\theta_{i+1}\right]+\\ +\dfrac{a(s_i)}{h_i+h_{i-1}}\left\{(\theta_{i+1}-\theta_{i-1})-\dfrac{d_i}{h_i}\left[\left(1+\dfrac{d_i}{h_{i-1}}\right)\theta_{i-1}-\left(2+\dfrac{d_i}{h_{i-1}}\right)\theta_i+\theta_{i+1}\right]\right\}+b(s_i)\theta_i\end{array}\right\}=f(s_i).$$

Arranging the above equation in three-term relation, we have:

$$L_i\theta_{i-1}+C_i\theta_i+U_i\theta_{i+1}=F_i \quad \text{for} \quad i=1,2,\ldots N-1. \tag{3.6}$$

Here

$$L_i=\frac{1}{h_i+h_{i-1}}\left[\frac{2}{h_i}\left(\varepsilon-a(s_i)\frac{d_i}{2}\right)\left(1+\frac{d_i}{h_{i-1}}\right)-a(s_i)\right],$$

$$C_i=\frac{1}{h_i+h_{i-1}}\left[b(s_i)(h_i+h_{i-1})-\frac{2}{h_i}\left(\varepsilon-a(s_i)\frac{d_i}{2}\right)\left(2+\frac{d_i}{h_{i-1}}\right)\right],$$

$$U_i=\frac{1}{h_i+h_{i-1}}\left[\frac{2}{h_i}\left(\varepsilon-a(s_i)\frac{d_i}{2}\right)+a(s_i)\right].$$

4. Mesh selection strategy

Let N be the number of grid points in the domain. Let $d_i=d=h_i-h_{i-1}$ be the common grid difference. Then

$$\begin{aligned}s_N-s_0&=(s_N-s_{N-1})+(s_{N-1}-s_{N-2})+\ldots\ldots+(s_1-s_0)=\\ &=\{h_0+(N-1)d\}+\{h_0+(N-2)d\}+\ldots+h_0=\\ &=\{(N-1)+(N-2)+\ldots\ldots+1\}d+Nh_0=\frac{1}{2}N(N-1)d+Nh_0,\end{aligned}$$

this gives $\quad d_i=\dfrac{2(1-Nh_0)}{N(N-1)}$.

Therefore, d is chosen from the above equation and subsequent h_i's can be acquired by $h_i=h_{i-1}+d$, $i=1,2,\ldots,N$.

5. Uniform convergence of the scheme

Let the problem Eq. (2.4) be denoted by Q_ε and the corresponding discretized problem be denoted by Q_ε^N, i.e.,

$$Q_\varepsilon=\begin{cases}\varepsilon\theta''+a(s)\theta'+b(s)\theta(s)=f(s) \text{ with}\\ \theta(0)=\varphi(0), \qquad\qquad \theta(1)=\varphi(1).\end{cases}$$

and

$$Q_\varepsilon^N = \begin{cases} \varepsilon\Delta^2\theta(s_i) + a(s_i)\Delta\theta(s_i) + b(s_i)\theta(s_i) = f(s_i) \\ \text{with } \theta(0) = \varphi(0), \qquad \theta(1) = \varphi(1). \end{cases}$$

Let π_ε be the operator corresponding to the continuous problem Q_ε and π_ε^N be the operator corresponding to the problem Q_ε^N, i.e.,

$$\pi_\varepsilon = \varepsilon\frac{d^2}{ds^2} + a(s)\frac{d}{ds} + b(s) \quad \text{and} \quad \pi_\varepsilon^N = \varepsilon\Delta^2 + a(s_i)\Delta + b(s_i)$$

where:

$$\Delta^2\theta(s_i) = \frac{2}{h_i(h_i + h_{i-1})}\left[\left(1 + \frac{d_i}{h_{i-1}}\right)\theta_{i-1} - \left(2 + \frac{d_i}{h_{i-1}}\right)\theta_i + \theta_{i+1}\right],$$

$$\Delta\theta(s_i) = \frac{1}{h_i + h_{i-1}}\left\{(\theta_{i+1} - \theta_{i-1}) - \frac{d_i}{h_i}\left[\left(1 + \frac{d_i}{h_{i-1}}\right)\theta_{i-1} - \left(2 + \frac{d_i}{h_{i-1}}\right)\theta_i + \theta_{i+1}\right]\right\}.$$

Uniform convergence of the method will be verified using the discrete minimum principle and the following lemmas.

Lemma 1. Discrete Minimum Principle: Suppose the grid function satisfies $\chi_0 \geq 0$ and $\chi_N \geq 0$. Then $\pi_\varepsilon^N \chi_i \leq 0$ for $0 \leq i \leq N-1$ implies that $\chi_i \geq 0$ for all $0 \leq i \leq N$.

Proof. Suppose there exists m, $0 \leq m \leq N$ such that $\chi_m = \min\limits_{0 \leq i \leq N-1} \chi_i$ and $\chi_m < 0$. By the hypothesis $\chi_0 \geq 0$ and $\chi_N \geq 0$, therefore $m \notin \{0, 1\}$. For $1 \leq m \leq N$ we have:

$$\begin{aligned}
\pi_\varepsilon^N \chi_m &= \frac{2\varepsilon}{h_m(h_m + h_{m-1})}\left[\left(1 + \frac{d_i}{h_{m-1}}\right)\chi_{m-1} - \left(2 + \frac{d_i}{h_{m-1}}\right)\chi_m + \chi_{m+1}\right] + \\
&+ \frac{1}{h_m + h_{m-1}}\left\{(\chi_{m+1} - \chi_{m-1}) - \frac{d_i}{h_m}\left[\left(1 + \frac{d_i}{h_{m-1}}\right)\chi_{m-1} - \left(2 + \frac{d_i}{h_{m-1}}\right)\chi_m + \chi_{m+1}\right]\right\} + b_m\chi_m = \\
&= \frac{2\varepsilon}{h_m(h_m + h_{m-1})}\left[\left\{\left(1 + \frac{d_i}{h_{m-1}}\right)(\chi_{m-1} - \chi_m)\right\} + (\chi_{m+1} - \chi_m)\right] + \\
&+ \frac{1}{h_m + h_{m-1}}\left[(\chi_{m+1} - \chi_m) - (\chi_{m-1} - \chi_m)\right] + \\
&- \frac{d_i}{h_m(h_m + h_{m-1})}\left[\left(1 + \frac{d_i}{h_{m-1}}\right)(\chi_{m-1} - \chi_m) + (\chi_{m+1} - \chi_m)\right] + b_m\chi_m.
\end{aligned} \tag{5.1}$$

Then, we have $\chi_{m-1}-\chi_m \geq 0,\ \chi_{m+1}-\chi_m \geq 0$ and $b_m < 0$. Using these inequalities and Eq.(3.6), we get $\pi_\varepsilon^N \chi_i > 0$. Thus for $1 \leq m \leq N$, we have $\pi_\varepsilon^N \chi_i > 0$, which contradicts the hypothesis that $\pi_\varepsilon^N \chi_i \leq 0$ for $1 \leq i \leq N-1$.
Therefore our assumption that $\chi_m < 0$ is wrong which implies that $\chi_i \geq 0$ for all $0 \leq i \leq N$.
Lemma 2. Let χ_i be any grid function such that $\chi_0 = \chi_N = 0.$ Then

$$|\chi_i| \leq \frac{1}{\vartheta} \max_{1\leq j\leq N-1} \left|\pi_\varepsilon^N \chi_j\right|, \quad \text{for } 0 \leq i \leq N.$$

Proof. We introduce two barrier functions $\psi_i^\pm$ defined by:

$$\psi_i^\pm = \frac{1}{\vartheta} \max_{1\leq j\leq N-1} \left|\pi_\varepsilon^N \phi_j\right| + \phi_i = L + \phi_i, \quad \text{for } 1 \leq i \leq N.$$

Then

$$\psi_0^\pm = L + \phi_0 = L > 0,\ \psi_N^\pm = L + \phi_N = L > 0 \quad \text{for} \quad 0 \leq i \leq N.$$

Now

$$\begin{aligned}
\pi_\varepsilon^N \psi_i^\pm &= \varepsilon \Delta^2 \psi_i^\pm + a(s_i)\Delta\psi_i^\pm + b(s_i)\psi_i^\pm = \\
&= \varepsilon\Delta^2(L \pm \chi_i) + a(s_i)\Delta(L \pm \chi_i) + b(s_i)(L \pm \chi_i) = \\
&= \pi_\varepsilon^N \chi_i \pm L b(s_i) \geq \pi_\varepsilon^N \chi_i \pm L\vartheta \geq 0.
\end{aligned}$$

Therefore, by Lemma 1, we have $\psi_i^\pm \geq 0$, for $1 \leq i \leq N-1$ which substantiates the required conclusion.

Lemma 3. Let $s_0 = 0,\ s_N = 1,\ d_i = h_i - h_{i-1}$ be the common grid difference, $s_i = \sum_{m=0}^{i-1} h_m$, for $1 \leq i \leq N-1$ then,

$$h_i \leq \frac{3}{N}.$$

Proof. For a detailed proof of this lemma one can refer to [17].
Lemma 4. For every $\phi \in C^3(0,1)$, we have:

$$\left\| \left(\Delta^2 - \frac{d^2}{ds^2} \right) \phi \right\| \leq \frac{2}{N} \|\phi\|_3 \quad \text{where} \quad \|\phi_j\| = \sup_{s\in(0,1)} \left\|\phi_{(s)}^{(j)}\right\|.$$

Proof. One can refer to [17].
Lemma 5. Let θ be the solution of the BVP Eq.(2.4) and let $\theta = u_\varepsilon + v_\varepsilon$. For $0 \leq k \leq 3$ and for small ε, the functions $u_\varepsilon,\ v_\varepsilon$ and their derivatives satisfy the following:

$$\left\| u_\varepsilon^{(k)} \right\| \leq C\varepsilon^{2-k},$$

$$\|v_\varepsilon(x)\| \le C\exp\left(-\frac{Ms}{\varepsilon}\right), \quad s\in[0,1],$$

$$\left\|v_\varepsilon^{(k)}\right\| \le C\varepsilon^{-k}\exp\left(-\frac{Ms}{\varepsilon}\right), \quad s\in[0,1].$$

Proof. One can refer to [6].

Theorem 1. The solution Y_ε of the discrete problem Q_ε^N and the solution θ_ε of the continuous problem Q_ε satisfy the following ε – uniform error estimate;

$$\sup_{0<\varepsilon\le 1} \|Y_\varepsilon - \theta_\varepsilon\| \le CN^{-1}(\ln N)^2, \tag{5.2}$$

where C is a positive constant unaffected by ε.

Proof. Decompose the solution Y_ε into regular (R_ε) and singular (W_ε) parts. Thus $Y_\varepsilon = R_\varepsilon + W_\varepsilon$ where R_ε is the solution of the non-homogeneous problem

$$\pi_\varepsilon^N R_\varepsilon = f, \quad R_\varepsilon(0) = r_\varepsilon(0), \quad R_\varepsilon(1) = r_\varepsilon(1) \tag{5.3}$$

and W_ε is the solution of the homogeneous problem

$$\pi_\varepsilon^N W_\varepsilon = 0, \quad W_\varepsilon(0) = w_\varepsilon(0), \quad W_\varepsilon(1) = w_\varepsilon(1). \tag{5.4}$$

Here r_ε and w_ε are the regular and singular parts of continuous problem Q_ε so that $\theta_\varepsilon = r_\varepsilon + w_\varepsilon$.
The error may be written in the form $Y_\varepsilon - \theta_\varepsilon = R_\varepsilon - r_\varepsilon + W_\varepsilon - w_\varepsilon$ it gives:

$$Y_\varepsilon - \theta_\varepsilon \le R_\varepsilon - r_\varepsilon + W_\varepsilon - w_\varepsilon. \tag{5.5}$$

As a conclusion, the error estimation in the regular and singular parts of the solution can be separated. Now we can evaluate the error for the regular part.

$$\pi_\varepsilon^N (R_\varepsilon - r_\varepsilon)(s_i) = f(s_i) - \pi_\varepsilon^N r_\varepsilon(s_i) = \left(\pi_\varepsilon - \pi_\varepsilon^N\right) r_\varepsilon = \varepsilon\left(\frac{d^2}{ds^2} - \Delta^2\right) r_\varepsilon + a(s_i)\left(\frac{d}{ds} - \Delta\right) r_\varepsilon. \tag{5.6}$$

Let $s_i \in [0,1]$. Then for any $\phi \in C^3(0,1)$ using Lemma 4, we have:

$$\left\|\left(\Delta^2 - \frac{d^2}{ds^2}\right)\phi\right\| \le \frac{2}{N}\|\phi_3\|$$

also, we obtained

$$\left\|\left(\Delta - \frac{d}{ds}\right)\phi \le \right\| \frac{3}{N^2} \|\phi\|_3.$$

Using these results in Eq.(5.6), we get

$$\left\|\pi_{\varepsilon}^{N}\left(R_{\varepsilon}-r_{\varepsilon}\right)\left(s_{i}\right)\right\| \leq \frac{2}{N} \varepsilon\left\|r_{\varepsilon}\right\|_{3}.$$

Using Lemma 5, for the estimation $r^{(3)}$ yields

$$\left\|\pi_{\varepsilon}^{N}\left(R_{\varepsilon}-r_{\varepsilon}\right)\left(s_{i}\right)\right\| \leq C N^{-1}. \tag{5.7}$$

Using inequality Lemma 1, to the grid function $\left(R_{\varepsilon}-r_{\varepsilon}\right)\left(s_{i}\right)$ gives

$$\left\|\left(R_{\varepsilon}-r_{\varepsilon}\right)\left(s_{i}\right)\right\| \leq \vartheta^{-1} \max_{1 \leq j \leq N-1}\left|\pi_{\varepsilon}^{N}\left(R_{\varepsilon}-r_{\varepsilon}\right)\left(s_{i}\right)\right|. \tag{5.8}$$

Using inequality Eq. (5.7) in inequality Eq.(5.8), we get

$$\left\|\left(R_{\varepsilon}-r_{\varepsilon}\right)\right\| \leq C N^{-1}. \tag{5.9}$$

Now by the same arguments as that for the regular part, the error estimate for the singular part of the solution is given by:

$$\left\|\pi_{\varepsilon}^{N}\left(W_{\varepsilon}-w_{\varepsilon}\right)\left(s_{i}\right)\right\| \leq \frac{2}{N} \varepsilon\left\|w_{\varepsilon}\right\|_{3}.$$

Using Lemma 5 for the estimation $w^{(3)}$ yields

$$\left\|\pi_{\varepsilon}^{N}\left(W_{\varepsilon}-w_{\varepsilon}\right)\left(s_{i}\right)\right\| \leq C \varepsilon^{-2} N^{-1}.$$

But in this case $\varepsilon^{-1} \leq C \ln(N)$, so the above inequality reduces to:

$$\left\|\pi_{\varepsilon}^{N}\left(W_{\varepsilon}-w_{\varepsilon}\right)\left(s_{i}\right)\right\| \leq C N^{-1}(\ln N)^{2}.$$

Using inequality Lemma 1 to the grid function $\left(W_{\varepsilon}-w_{\varepsilon}\right)\left(s_{i}\right)$ gives:

$$\left\|\left(W_{\varepsilon}-w_{\varepsilon}\right)\left(s_{i}\right)\right\| \leq C N^{-1}(\ln N)^{2}. \tag{5.10}$$

Combining the inequalities Eq.(5.5) to Eq.(5.10) gives the desired result Eq.(5.2).

6. Numerical illustrations

To verify the applicability of the method, model problems of the types Eqs (2.1)-(2.2) are considered. The exact solution of the problem is $\theta(s)=c_{1} e^{m_{1} s}+c_{2} e^{m_{2} s}+\dfrac{f}{C}$

where

$$C = b + c + d\,, \qquad c_1 = \frac{\left[-f + \gamma C + e^{m_2}\left(f - fC\right)\right]}{\left(e^{m_1} - e^{m_2}\right)C_1},$$

$$c_2 = \frac{\left[f - yC + e^{m_1}\left(-f + fC\right)\right]}{\left(e^{m_1} - e^{m_2}\right)C}, \qquad m_1 = \frac{\left[-(p - q\delta + v\eta) + \sqrt{(p - q\delta + v\eta)^2 - 4\varepsilon C}\right]}{2\varepsilon},$$

$$m_2 = \frac{\left[-(p - q\delta + v\eta) - \sqrt{(p - q\delta + v\eta)^2 - 4\varepsilon C}\right]}{2\varepsilon}.$$

Example 1. $\varepsilon\theta''(s) + \theta' + 2\theta(s - \delta) - 3\theta = 0$ with $\theta(s) = 1, -\delta \le s \le 0,\ \theta(s) = 1,\ 1 \le s \le 1 + \eta$.

Example 2. $\varepsilon\theta''(s) + \theta' - 3\theta + 2\theta(s + \eta) = 0$ with $\theta(s) = 1, -\delta \le s \le 0,\ \theta(s) = 1,\ 1 \le s \le 1 + \eta$.

Example 3. $\varepsilon\theta''(s) + \theta' - 2\theta(s - \delta) - 5\theta + \theta(s + \eta) = 0$ with $\theta(s) = 1, -\delta \le s \le 0,\ \theta(s) = 1,\ 1 \le s \le 1 + \eta$.

Example 4. $\varepsilon\theta''(s) - \theta' - 2\theta(s - \delta) + \theta = 0$ with $\theta(s) = 1, -\delta \le s \le 0, \theta(s) = -1,\ 1 \le s \le 1 + \eta$.

Example 5. $\varepsilon\theta''(s) - \theta' + \theta - 2\theta(s + \eta) = 0$ with $\theta(s) = 1, -\delta \le s \le 0,\ \theta(s) = -1,\ 1 \le s \le 1 + \eta$.

Example 6. $\varepsilon\theta''(s) - \theta' - 2\theta(s - \delta) + \theta - 2\theta(s + \eta) = 0$ with $\theta(s) = 1,\ -\delta \le s \le 0,\ \theta(s) = -1,\ 1 \le s \le 1 + \eta$.

7. Conclusion

The equation having a layer structure with small shifts is solved using a difference technique on a nonuniform grid. Finite difference estimates are obtained for the first and second-order derivatives using the nonuniform grid.

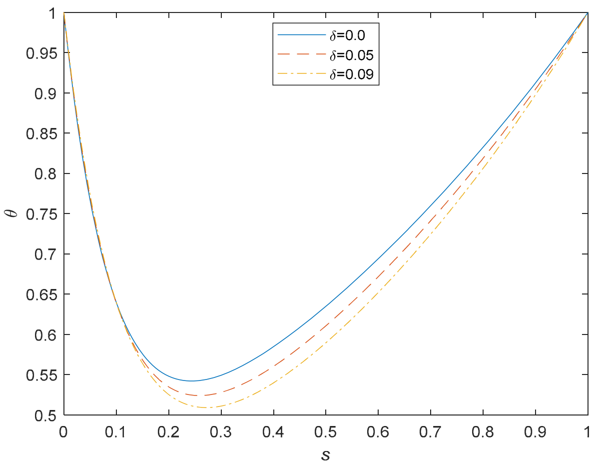

Fig.1. Layer profile in Example 1 with $\varepsilon = 0.1$.

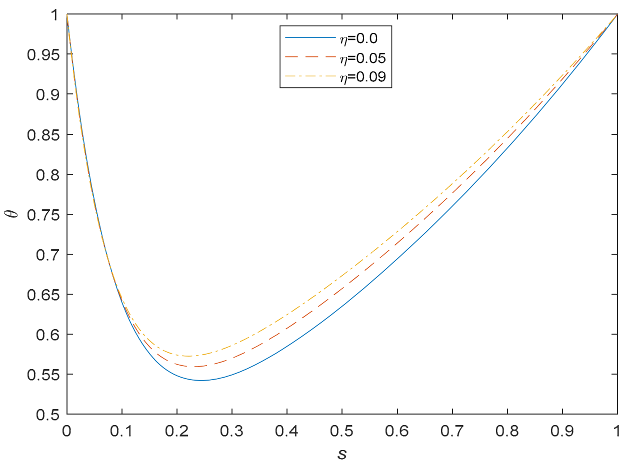

Fig.2. Layer profile in Example 2 with $\varepsilon = 0.1$.

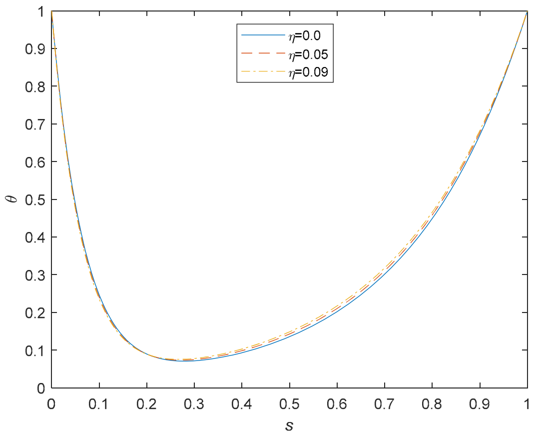

Fig.3. Layer profile in Example 3 with $\varepsilon = 0.1, \delta = 0.5\varepsilon$.

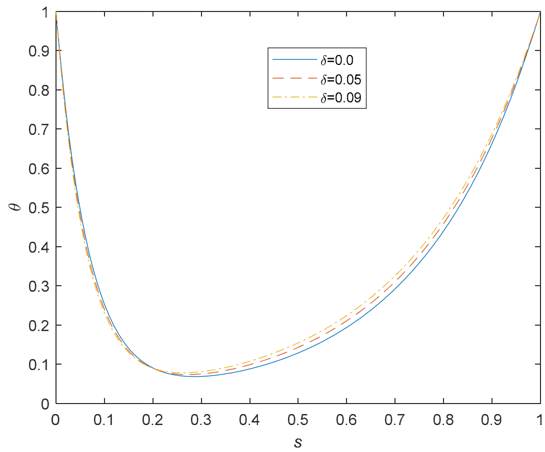

Fig.4. Layer profile in Example 3 with $\varepsilon = 0.1, \eta = 0.5\varepsilon$.

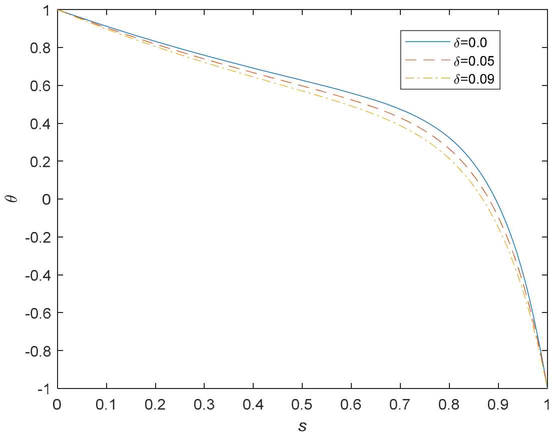

Fig.5. Layer profile in Example 4 with $\varepsilon = 0.1$.

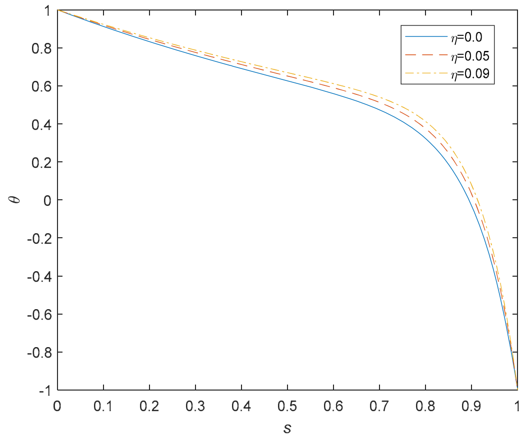

Fig.6. Layer profile in Example 5 with $\varepsilon = 0.1$.

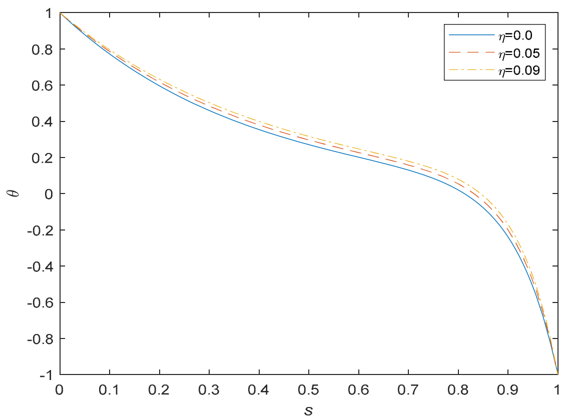

Fig.7. Layer profile in Example 6 with $\varepsilon = 0.1, \delta = 0.5\varepsilon$.

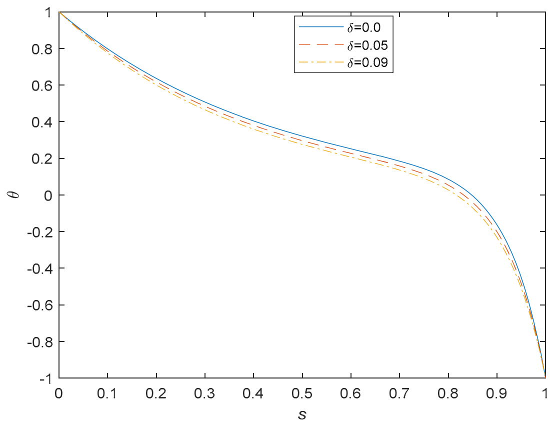

Fig.8. Layer profile in Example 6 with $\varepsilon = 0.1$, $\eta = 0.5\varepsilon$.

Making use of these approximations, the given equation is discretized and solved using the tridiagonal algorithm. Convergence of the scheme is established. Multiple numerical examples are illustrated to validate the method. MATLAB software is used to design the codes for the solution of the examples. For Examples 1-6, the maximum absolute errors (MAEs) in the solutions are listed in Tabs 1-6. The proposed method was shown to be more accurate than the methods in [24] and [12] when comparing the computed errors. The rate of convergence of the scheme for the examples is calculated and shown in Tab.7. Figures 1-8 show the layer structure to the examples for a various value of the shift parameters. Using Figs 1-4, it is noticed that, when δ increased, the width of the left end boundary layer decreases and it is increased when η is increased. From Figs 5-8, we noticed that when δ increased the size of the right end boundary layer increases and it is decreased when η is increased.

Table 1. MAEs in Example 1 with $\varepsilon = 0.1$.

$N \rightarrow$	32	128	512
$\delta\downarrow$	Suggested method		
0.00	2.2648e-03	1.2536e-04	5.9442e-06
0.05	2.0935e-03	1.1586e-04	5.3476e-06
0.09	1.9443e-03	1.0735e-04	4.8437e-06
$\delta\downarrow$	*Results in [9]*		
0.00	3.7007e-02	9.5467e-03	2.1450e-03
0.05	3.6405e-02	9.2466e-03	2.0299e-03
0.09	3.5566e-02	8.9517e-03	1.9248e-03
$\delta\downarrow$	Results in [1]		
0.00	3.5537e-03	9.1770e-04	2.3113e-04
0.05	3.8619e-03	9.9278e-04	2.4977e-04
0.09	4.1191e-03	1.0557e-03	2.6536e-04

Table 2. MAEs in Example 2 with $\varepsilon = 0.1$.

$N \rightarrow$	32	128	512
$\eta\downarrow$	Suggested method		
0.00	2.2648e-03	1.2536e-04	5.9442e-06
0.05	2.4169e-03	1.3371e-04	6.5072e-06
0.09	2.5154e-03	1.3970e-04	6.9362e-06
$\eta\downarrow$	*Results in [9]*		
0.00	3.7007e-02	9.5467e-03	2.1450e-03
0.05	3.7270e-02	9.7965e-03	2.2447e-03
0.09	3.7238e-02	9.9628e-03	4.5869e-03
$\eta\downarrow$	*Results in [1]*		
0.00	2.8330e-03	7.4107e-04	1.8720e-04
0.05	2.6115e-03	6.8579e-04	1.7341e-04
0.09	2.4443e-03	6.4520e-04	1.6328e-04

Table 3. MAE for Example 3 with $\varepsilon = 0.1$.

$N \rightarrow$	32	128	512
$\delta \downarrow$	$\eta = 0.05$	Suggested method	
0.00	3.1908e-03	1.7721e-04	8.1741e-06
0.05	3.5660e-03	1.9754e-04	9.4574e-06
0.09	3.8696e-03	2.1406e-04	1.0534e-05
$\eta \downarrow$	$\delta = 0.05$		
0.00	3.3775e-03	1.8734e-04	8.8067e-06
0.05	3.5660e-03	1.9754e-04	9.4574e-06
0.09	3.7175e-03	2.0571e-04	9.9905e-06
Results in [1]			
$\delta \downarrow$	$\eta = 0.05$		
0.00	1.7890e-02	4.5754e-03	1.1494e-03
0.05	1.7272e-02	4.4321e-03	1.1147e-03
0.09	1.6748e-02	4.3186e-03	1.0870e-03
$\eta \downarrow$	$\delta = 0.05$		
0.00	1.7587e-02	4.5038e-03	1.1321e-03
0.05	1.7272e-02	4.4321e-03	1.1147e-03
0.09	1.7013e-02	4.3752e-03	1.1008e-03
Results in [9]			
$\delta \downarrow$	$\eta = 0.05$		
0.00	3.4534e-02	1.1643e-02	3.0046e-03
0.05	3.8231e-02	1.2958e-02	3.3513e-03
0.09	4.1108e-02	1.4001e-02	3.6292e-03
$\eta \downarrow$	$\delta = 0.05$		
0.00	3.6404e-02	1.2294e-02	3.1778e-03
0.05	3.8231e-02	1.2958e-02	3.3513e-03
0.09	3.9658e-02	1.3483e-02	3.4905e-03

Table 4. MAEs for Example 4 for with $\varepsilon = 0.1$

$N \rightarrow$	32	128	512
$\delta \downarrow$	Suggested method		
0.00	9.9096e-03	5.5551e-04	2.3088e-05
0.05	7.2235e-03	4.0487e-04	1.7063e-05
0.09	5.4742e-03	3.0372e-04	1.2923e-05
Results in [9]			
0.00	4.6789e-02	1.7279e-02	4.4308e-03
0.05	3.8283e-02	1.4877e-02	3.8067e-03
0.09	3.1492e-02	1.2993e-02	3.3193e-03
Results in [1]			
0.00	9.3435e-03	2.4536e-03	6.2174e-04
0.05	1.0039e-02	2.6180e-03	6.6231e-04
0.09	1.0571e-02	2.7569e-03	6.9686e-04

Table 5. MAEs in Example 5 with $\varepsilon = 0.1$.

$N \rightarrow$	32	128	512
$\eta \downarrow$ Suggested method			
0.00	9.9096e-03	5.5551e-04	2.3088e-05
0.05	1.3384e-02	7.2751e-04	3.0086e-05
0.09	1.6586e-02	8.8665e-04	3.6388e-05
Results in [9]			
0.00	4.6789e-02	1.7279e-02	4.4308e-03
0.05	5.5164e-02	1.9725e-02	5.0676e-03
0.09	6.1682e-02	2.1696e-02	5.5845e-03
Results in [1]			
0.00	9.3435e-03	2.4536e-03	6.2174e-04
0.05	8.7029e-03	2.3021e-03	5.8424e-04
0.09	8.2900e-03	2.1895e-03	5.5647e-04

Table 6. MAE in Example 6 with $\varepsilon = 0.1$.

$N \rightarrow$	32	128	512
$\delta \downarrow$	$\eta = 0.05$ Suggested method		
0.00	9.2888e-03	4.9625e-04	2.0550e-05
0.05	6.7830e-03	3.6849e-04	1.5464e-05
0.09	5.0656e-03	2.8006e-04	1.1897e-05
$\eta \downarrow$	$\delta = 0.05$		
0.00	4.6748e-03	2.5982e-04	1.1073e-05
0.05	6.7830e-03	3.6849e-04	1.5464e-05
0.09	8.7549e-03	4.6934e-04	1.9478e-05
Results in [9]			
$\delta \downarrow$	$\eta = 0.05$		
0.00	3.6850e-02	1.3316e-02	3.4288e-03
0.05	3.2184e-02	1.1671e-02	2.9957e-03
0.09	2.8503e-02	1.0389e-02	2.6637e-03
$\eta \downarrow$	$\delta = 0.05$		
0.00	2.7595e-02	1.0078e-02	2.5829e-03
0.05	3.2184e-02	1.1671e-02	2.9957e-03
0.09	3.5914e-02	1.2973e-02	3.3404e-03
Results in [1]			
$\delta \downarrow$	$\eta = 0.05$		
0.00	1.6643e-02	4.3793e-03	1.1118e-03
0.05	1.6949e-02	4.4649e-03	1.1320e-03
0.09	1.7233e-02	4.5266e-03	1.1463e-03
$\eta \downarrow$	$\delta = 0.05$		
0.00	1.7317e-02	4.5402e-03	1.1496e-03
0.05	1.6949e-02	4.4649e-03	1.1320e-03
0.09	1.6711e-02	4.3982e-03	1.1160e-03

Table 7. Rate of Convergence with $\varepsilon = 0.1$.

$N \rightarrow$	32	128	512
$\delta \downarrow$	*Example 1*		
0.00	2.0760	2.1668	1.8917
0.05	2.0739	2.1733	2.0103
0.09	2.0756	2.1789	2.1207
$\eta \downarrow$	*Example 2*		
0.00	2.0760	2.1668	1.8917
0.05	2.0768	2.1602	1.7892
0.09	2.0718	2.1552	1.7161
$\delta \downarrow$	$\eta = 0.05$ *Example 3*		
0.00	2.0674	2.1732	2.0209
0.05	2.0757	2.1643	1.8589
0.09	2.0772	2.1572	1.7543
$\eta \downarrow$	$\delta = 0.05$		
0.00	2.0715	2.1689	1.9348
0.05	2.0757	2.1643	1.8589
0.09	2.0767	2.1604	1.8043
$\delta \downarrow$	*Example 4*		
0.00	2.0434	2.1994	2.6339
0.05	2.0417	2.1926	2.5513
0.09	2.0685	2.1933	2.4645
$\eta \downarrow$	*Example 5*		
0.00	2.0434	2.1994	2.6339
0.05	2.0899	2.1969	2.6977
0.09	2.1282	2.2022	2.7391
$\delta \downarrow$	$\eta = 0.05$ Example 6		
0.00	2.1307	2.0957	2.6577
0.05	2.1004	2.1958	2.5744
0.09	2.0675	2.1094	2.4845
$\eta \downarrow$	$\delta = 0.05$		
0.00	2.0596	2.1929	2.4576
0.05	2.1004	2.1958	2.5744
0.09	2.1292	2.2001	2.6432

Nomenclature

d_i – grid difference

h_i – mesh size

N – number of sub intervals

s – independent variable

s_i – mesh points

δ – delay parameter

ε – perturbation parameter

η – advance parameter

θ – solution

References

[1] Kuang Y. (1993): *Delay Differential Equations with Applications in Population Dynamics.*– Mathematics in Science and Engineering, Academic Press Inc, Boston.

[2] Mackey C. and Glass L. (1977): *Oscillations and chaos in physiological control systems*.– *Science*, vol.197, pp.287-289.

[3] Martin A. and Raun S. (2001): *Predator-prey models with delay and prey harvesting*.– J. Math. Bio., vol.43, pp.247-267.

[4] Stein R.B. (1967): *Some models of neuronal variability.*– Biophys. J., vol.7, No.1, pp.37-68.

[5] Driver R.D. (1977): *Ordinary and Delay Differential Equations.*– Applied Mathematical Sciences*,* Springer-Verlag New York-Heidelberg-Berlin.

[6] El'sgol'ts L.E. and Norkin S.B. (1973): *Introduction to the theory and application of differential equations with deviating arguments*.– Mathematics in Science and Engineering, Academic Press.

[7] Bender C.M. and Orszag S. A. (1978): *Advanced Mathematical Methods for Scientists and Engineers*.− McGraw-Hill, New York.

[8] Doolan E.P., Miller J.J.H. and Schilders W.H.A. (1980): *Uniform Numerical Methods for Problems with Initial and Boundary Layers*.– Boole Press, Dublin.

[9] Kokotovic P.V., Khalil H.K. and Reilly J.O. (1986): *Singular perturbation methods in control analysis and design*.– McGraw-Hill, Academic Press.

[10] Miller J.J.H., Riordan E.O. and Shishkin I.G. (2012): *Fitted Numerical Methods for Singular Perturbation Problems*.– World Scientific Publishing, Singapore.

[11] O'Malley R.E. (1974): *Introduction to Singular Perturbations*.– Academic Press, New York.

[12] Kadalbajoo M.K., Sharma K.K. (2005): *Numerical treatment of mathematical model arising from a model of neuronal variability.*– J. Mathematical Analysis and Applications, vol.307, No.2, pp.606-627.

[13] Kadalbajoo M.K. and Devendra Kumar (2010): *Variable mesh finite difference method for self-adjoint singularly perturbed two-point boundary value problems*.– J. Compu. Math., vol.25, No.5 pp.711-724.

[14] Lange C.G. and Miura R.M. (1985): *Singular perturbation analysis of boundary value problems for differential-difference equations III Turning point problems*.– SIAM. J. Appl. Math., vol.45, No.5, pp.708-734.

[15] Lange C.G. and Miura R.M. (1994): *Singular perturbation analysis of boundary-value problems for differential-difference equations V Small shifts with layer behaviour*.– SIAM. J. Appl. Math., vol.54, No.1, pp.249-272.

[16] Lange C.G. and Miura R.M. (1994): *Singular perturbation analysis of boundary-value problems for-difference equations VI Small shifts with rapid oscillations*.– SIAM. J. Appl. Math., vol.54, No.1, pp.273-283.

[17] Farshid Mirzaee and Nasrin Samadyar (2019): *Numerical solution of time fractional stochastic Korteweg-de Vries equation via implicit meshless approach.*– Iranian Journal of Science and Technology, Transactions A: Science, vol.43, No.6, pp.2905-2912.

[18] Farshid Mirzaee and Nasrin Samadyar (2020): *Combination of finite difference method and meshless method based on radial basis functions to solve fractional stochastic advection-diffusion equations.*– Engineering with Computers, vol.36, pp.673-686.

[19] Farshid Mirzaee and Seyede Fatemeh Hoseini (2013): *Solving singularly perturbed differential-difference equations arising in science and engineering with Fibonacci polynomials.*– Results in Physics, vol.3, pp.134-141.

[20] Lakshmi Sirisha, Phaneendra K. and Reddy Y.N. (2018): *Mixed finite difference method for singularly perturbed differential difference equations with mixed shifts via domain decomposition.*– Ain Shams Engineering Journal, vol.9, No.4, pp.647-654.

[21] Phaneendra K., Kumara Swamy D. and Reddy Y.N. (2018): *Computational method for singularly perturbed delay differential equations with twin layers or oscillatory behaviour.*– Khayyam J. Math., vol.4, No.2, pp.110-122.

[22] Ravi Kanth A.S.V. and Murali Mohan Kumar P. (2017): *A numerical approach for solving singularly perturbed convection delay problems via exponentially fitted spline method*.– Calcolo, vol.54, pp.943-961.

[23] Xuefei He and Kun Wang (2018): *New finite difference methods for singularly perturbed convection-diffusion equations.*– Taiwanese Journal of Mathematics, vol.22, No.4, pp.949-978.

[24] Adilaxmi M. (2021): *Gaussian quadrature method for solving differential difference equations having boundary layers*.– J. Math. Comput. Sci., vol.11, No.3, pp.2814-2833.

Received: November 11, 2021
Revised: January 25, 2022